BSMA: Scalable LoRa networks using full duplex gateways

Raghav Subbaraman[†], Yeswanth Guntupalli[†], Shruti Jain[†], Rohit Kumar[†],
Krishna Chintalapudi[§], Dinesh Bharadia[†]
[†]University of California San Diego, [§]Microsoft Research
USA
{rsubbaraman,yguntupa,shjain,rokumar,dineshb}@eng.ucsd.edu,krchinta@microsoft.com

Abstract

With its ability to communicate long distances, LoRa promises city-scale IoT deployments for smart city applications. This long-range, however, also increases contention as many thousands of devices are connected. Recently, CSMA has been proposed as a viable MAC for resolving contention in LoRa networks. *In this paper, supported by measurements, we demonstrate that CSMA is ineffective in urban deployments.* While gateways stationed at rooftops enjoy a long communication range, 70% of the devices placed at street level fail to sense each others' transmissions and remain hidden, owing to obstructions by tall structures. *We present Busy Signal Multiple Access (BSMA), where the LoRa gateway transmits a downlink busy signal while receiving an uplink transmission.* The IoT devices defer uplink transmissions while a busy signal is present. Practically viable BSMA requires a full-duplex LoRa gateway – i.e., a gateway that can simultaneously receive and transmit in the same channel. *We develop the first full Duplex LoRa gateway in the 915 MHz ISM band, overcoming challenges that arise from a 9× greater delay spread and the need for 1000× greater self-interference cancellation.* Our implementation works with COTS LoRa devices and improves network capacity by 100% compared to CSMA in bursty loads while being fair to all IoT devices near and far.

CCS Concepts

• **Networks → Link-layer protocols**.

ACM Reference Format:
Raghav Subbaraman, Yeswanth Guntupalli, Shruti Jain, Rohit Kumar, Krishna Chintalapudi, Dinesh Bharadia. 2022. BSMA: Scalable LoRa networks using full duplex gateways. In *The 28th Annual International Conference On Mobile Computing And Networking (ACM MobiCom '22), October 17–21, 2022, Sydney, NSW, Australia.* ACM, New York, NY, USA, 14 pages. https://doi.org/10.1145/3495243.3560544

1 Introduction

LoRa [1], owing to its long communication range and low power consumption, is being deployed in cities to enable smart city applications, e.g., smart metering, smart parking, fire alarms, and critical infrastructure monitoring. Consequently, as LoRa gains popularity, its vast reach coupled with uncoordinated network deployments culminates in severe contention amongst devices spread across several square kilometers of area, thus undermining its network reliability and throughput [2, 3]. Lost packets require these low-power devices to expend additional energy in re-transmissions. An efficient and fair Medium Access Control (MAC) is thus paramount to LoRa's success.

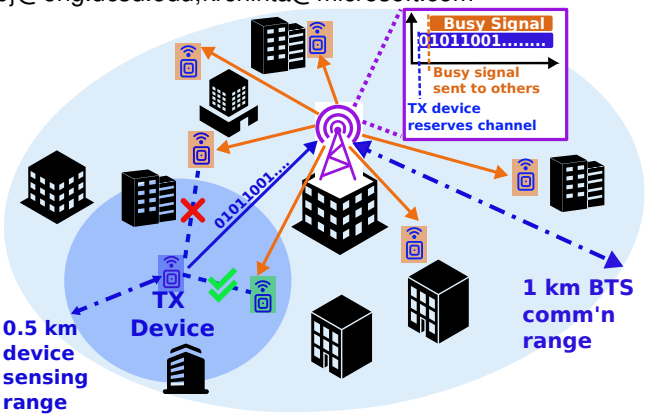

Figure 1: The sensing channels are significantly inferior to communication channels in urban wide-area deployments. BSMA alleviates the hidden node problem by transmitting a Busy Signal during ongoing uplink transmissions.

While current networks use ALOHA [2], attempts at other MAC designs for LoRa have followed in WiFi's footsteps. Akin to Carrier Sensing (CS) used in CSMA, LoRa chips are capable of Channel Activity Detection (CAD). LoRa devices can use CAD to sense ongoing communication and defer their transmissions to avoid packet collisions. Recently, a few LoRa deployment studies [4–6] have demonstrated that CAD-based CSMA can improve network capacity by reducing wasteful packet collisions.

In this paper, guided by measurements in an urban deployment, we show that LoRa devices using CAD fail to detect uplink transmissions in 70% of the cases leading to a proliferation of hidden nodes. We show that this hidden node problem severely undermines CSMA's effectiveness, reducing its network capacity by ≈50%. This failure of CAD as a practical sensing mechanism stems from the nature of urban wide-area LoRa deployments. Through our measurement study (Section 2) in an urban area, we find the gateway has a reliable communication range of about 1 km to/from the IoT devices when stationed 20-30 m above the ground on a building's roof (Figure 1). However, the devices are unable to sense each others' uplink transmissions when separated by >500m, due to buildings and other obstructions at the ground level. Consequently, CAD fails to detect and avoid ≈70% of packet collisions (determined by the ratio of sensing to communication areas $\approx 1^2 - .5^2$).

In this paper, we propose in-band Busy Signal Multiple Access (BSMA) for LoRa. In BSMA, immediately upon detecting an uplink transmission, the gateway transmits a LoRa busy signal packet in

ACM MobiCom '22, October 17–21, 2022, Sydney, NSW, Australia

ACM ISBN 978-1-4503-9181-8/22/10…$15.00
https://doi.org/10.1145/3495243.3560544

the same channel. This busy signal lasts the duration of the uplink transmission (Figure 1). In BSMA, all LoRa devices follow standard CSMA protocol. Since all LoRa devices in the network can reliably sense the gateway's continuous busy signal, even if they wake up sporadically, they defer their transmissions to avoid collision (following CSMA) with the ongoing uplink transmission. Thus, BSMA resolves contention and avoids the hidden node problem.

The idea of using busy-signal to circumvent hidden nodes is first proposed in [7] and later in the context of WiFi [8–10]. All of these approaches suggest transmitting the busy signal over a separate channel. Consequently, these solutions neither saw widespread adoption nor significant gains since they use an additional channel that the gateway could otherwise use for communication [11, 12]. *Our design obviates the need for this additional channel by using an in-band full duplex LoRa gateway.* A key contribution of this paper is the design of *the first in-band full-duplex LoRa gateway that can simultaneously receive and transmit LoRa packets over the same channel.* Our full duplex gateway can function with COTS LoRa IoT end devices without requiring modifications.

While Full duplex radios have been developed and studied extensively in the past for 2.4 GHz WiFi [13–15], developing a LoRa compliant full duplex gateway at 915 MHz presents two unique challenges. The first is designing for the extreme receiver sensitivity of COTS LoRa devices as low as -120dBm (for perspective, sensitivity is -90dbm for WiFi, i.e., 1000× worse than LoRa). To achieve full-duplex, one needs to cancel the self-interference to the noise floor (Section 4), which requires an analog self-interference cancellation circuit that can provide cancellation of 100 dB (10 decimal places) – almost 1000× greater than hitherto achieved. Second, the superior propagation characteristics of RF signals at 915 MHz compared to 2.4 GHz results in 9× prolonged self-interference multipath reflections (large delay spread). To provide perspective, while self-interference multipath reflections last only 5 ns in 2.4 GHz for 50 dB signal loss, they last over 45 ns (9× more) in 900 MHz (Section 4) for the same amount of signal loss.

The typical analog cancellation approach used to meet the stringent requirements is using a circuit with physical wires to recreate the delay and vary amplitude and phase to match each path of the self-interference and cancel it [13, 16]. Canceling long delays at 900 MHz, therefore, would require (9×) long physical wires in the analog circuit impacting its cost, form factor, and cancellation performance, making it impractical to build.

In this paper, instead of recreating the true multipath delays of self-interference in the analog cancellation circuit, we show that we can approximate the long duration of the multipath using two shorter delays. Our key insight is that for narrow bandwidth, the two short delays, if combined properly, can mimic large delays. Based on this insight and through extensive channel measurement and experimentation, we show that for narrowband LoRa, the 45 ns multipath can be approximated accurately by using a set of 2 shorter delays between 8 and 15 ns. This *Short Delay Approximation* approach lets us use shorter wires that make the analog cancellation circuit design practical. In combination with antenna isolation, we achieve the required 100 dB of RF cancellation despite the high delay spread.

LoRa receivers are sensitive even below the noise floor due to the chirp-spread-spectrum modulation [1]. While conventional analog and digital SIC approaches cancel signals to the noise floor, that is not enough in the case of LoRa. To address this, we develop a bespoke digital cancellation technique:*bin suppression*, taking advantage of the spread spectrum nature of the self-interference and suppressing sub-noise floor residue to obtain a total cancellation of 117.8 dB.

We fabricate an analog cancellation circuit, combining antenna isolation and digital cancellation, to achieve self-interference cancellation below the noise floor. Using the self-interference cancellation, we prototype the world's first full-duplex LoRa gateway with COTS devices and Software Defined Radio (SDR). We evaluate our system in an urban setting and with varying LoRa traffic loads. Our contributions and results are summarized below:

- We use our full duplex LoRa gateway to implement the BSMA MAC. Through experiments in outdoor deployments, emulations and simulations, we show that BSMA can provide up to 2× throughput and energy efficiency compared to conventional CSMA in urban environments where the fraction of hidden nodes can be as high as 70%. We further demonstrate that BSMA scales to thousands of nodes and multi-gateway deployments through simulations.
- We use our full duplex LoRa gateway to implement the BSMA MAC. Through experiments in outdoor deployments, emulations, and simulations, we show that BSMA can provide up to 2× throughput and energy efficiency compared to conventional CSMA in urban environments where the fraction of hidden nodes can be as high as 70%. We further demonstrate that BSMA scales to thousands of nodes and multi-gateway deployments through simulations.
- We develop a LoRa testbed based on open-source software to test various MAC protocols with standalone LoRa devices. The code-base for our simulations, hardware testbed and analog cancellation circuit design are open-sourced at **github.com/ucsdwcsng/bsma_lora**, to benefit cross-layer research in LoRa.

2 LoRa CAD Measurement Study

CSMA and many other protocols in LPWAN rely on channel activity detection (CAD) performed at IoT devices. In this section, we ask the question, *"How effective is LoRa's CAD as a channel sensing mechanism in urban environments?"* To answer this question, we perform CAD measurements in La Jolla, CA. Guided by our measurements, we simulate to predict the effect of the failure of CAD (hidden nodes) on CSMA's performance.

LoRa Primer: LoRa is a long-range, chirp spread spectrum modulation developed by Semtech [1], designed for wide area IoT applications such as smart cities. LoRa allows devices to tradeoff data rates to achieve longer ranges through various mechanisms – by increasing the duration of the chirps (parameterized by the spreading factor (SF)), the signal bandwidth (125 kHz-500 kHz), and the choice of coding rates. In a typical LoRa deployment, several hundred IoT devices spread across a large spatial extent (several km^2) transmit uplink messages at unpredictable times in response to physical events. LoRa devices predominantly use ALOHA [17] for channel access scheme [2, 18] where sensors transmit messages without coordination. As LoRa deployments grow in number and size, this uncoordinated access adversely affects network capacity due to

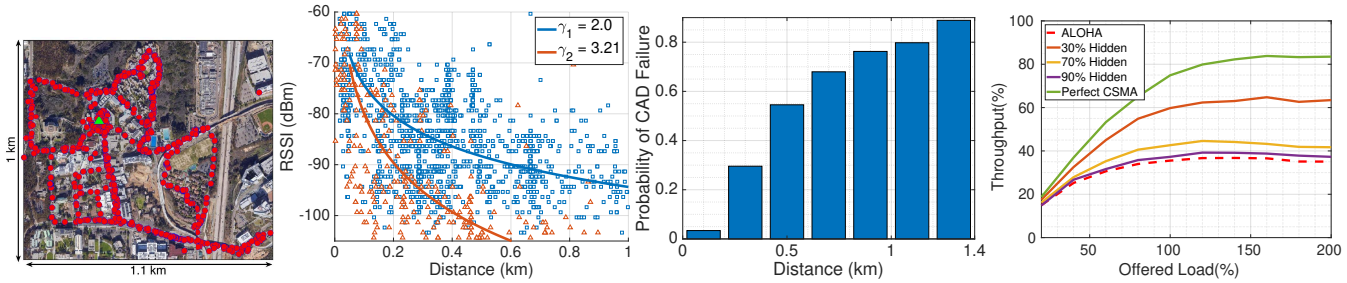

(a) (b) (c) (d)

Figure 2: (a) Circles represent sampling locations from our measurement study; the triangle is the gateway. (b) LDPL Model fit of gateway-device ($\gamma_1 = 2.0$, square) and device-device ($\gamma_2 = 3.21$, triangle) link RSSI with distance. The device-device link attenuates quicker than the gateway-device link with distance. (c) The probability of CAD Failure increases as the length of the device-device links increases, with the 67% average failure rate among two random device pairs. (d) Throughput Performance of CSMA with various CADFR percentages compared with ALOHA and Perfect CSMA. CSMA provides almost no improvement over ALOHA when the CADFR is $\geq$ 70%

packet collisions. LoRa optionally implements CAD, enabling devices to sense ongoing transmissions and avoid collisions using a CSMA-style MAC, similar to WiFi.

CAD Effectiveness Measurement Study: We define CAD Failure Rate (CADFR) as the likelihood that an uplink transmission from a device will not be detected by another even though both devices are within range of the gateway. To answer the question *"What is the expected CADFR in an urban environment?"*, we perform measurements at our university campus, with several multi-story buildings (ranging 10-30 m in height), houses, and streets. We deploy a COTS 915 MHz LoRa gateway [19] on the roof of a building at the height of ≈25m. Volunteers carrying a GPS-equipped LoRa IoT device walk/bike around the streets in the deployment terrain. In each measurement cycle, the gateway transmits a downlink message to each IoT device, requesting it to respond. The IoT device then responds with an uplink transmission to the gateway while other IoT devices listen. The gateway and the listening IoT devices record the uplink message's RSSI and its receipt time. RSSI is recorded even for packets with CRC failures since CAD relies only on preamble detection and not complete packet decoding. The gateway repeats the measurement cycle every 3 seconds. The collected data at all the IoT devices and gateway is processed at the end of the experiment to evaluate CAD failures. A CAD failure occurs when a listening IoT device completely misses the transmission, or the RSSI is below the CAD RSS threshold. In all our experiments, we use SF=8.

Uplink transmissions received from ≈1800 different locations comprise our study as depicted in Fig. 2(a). Fig. 2(b) plots the RSS of the uplink transmissions as a function of distance for these locations as well as a Log Distance Path Loss (LDPL) model [20] estimate. Based on Fig. 2(b), the approximate range of the gateway is about 1 km (as packet reception decreases to below 50% at -100dbm). A majority of LoRa gateway deployments, such as in the Helium LoRa network, are known to have hearing ranges within a few km [21] and agree with our measurement scenario. Fig. 2(b) also depicts the RSS for the same uplink transmissions as received at other sensor devices at the ground level and the corresponding LDPL model. The RSS decays significantly faster with distance at ground level than that at the gateway and has a range of around 500 m. Note that the maximum possible distance between devices is 2 km (network diameter) while the network range is 1 km.

We also measured the CADFR, i.e., a fraction of cases where IoT devices could not detect uplink transmissions from other devices. *The fraction of instances where a CAD failure occurred among all our measurements was found to be 67%.* To understand how CADFR depends on distance, Fig. 2(c) depicts the probability of CAD failure as a function of the distance between the devices on the street level. As seen from Fig. 2(c), the CADFR increases steadily with the distance between the devices and is > 60% for distances greater than 500m. Beyond 1.2 km, the CADFR is almost 100%. In a typical urban deployment, most of the devices will be apart by over 1 km and consequently hidden from each other.

Impact on CSMA: The inability to detect ongoing transmissions using CAD implies that IoT devices will not be able to avoid collisions while using CSMA. The spread spectrum nature of the LoRa PHY layer leads to a significantly higher *capture effect*, where in the event of a multi-packet collision, one of the collided transmissions is almost always correctly received [6]. the capture effect in WiFi is significantly different, where the capture effect only occurs when the signal strength difference between the collided transmissions exceeds a certain threshold (6-20 dB depending on the data rate [22, 23]) Fig. 2(d) depicts the CSMA network throughput for various CADFR values as a function of uplink traffic rate assuming perfect capture effect (at least one of the colliding packets is received correctly) evaluated using simulations. In Fig. 2(d), traffic is generated using a Poisson distribution. We normalize all values by the maximum possible network capacity of the channel. As seen in Fig. 2(d), as CADFR increases, CSMA approaches the performance of ALOHA and is only marginally better at a CADFR of 70%.

Conclusion: We arrive the following conclusions from our study:

- CAD in LoRa used to sense ongoing transmissions is not effective in urban settings, with a failure rate of almost 70%.
- The high CAD failure rate significantly undermines the performance of CSMA and reduces its utility

Since the gateway is able to hear all the transmitting devices, it is in the perfect position to notify all the IoT devices of an ongoing transmission.

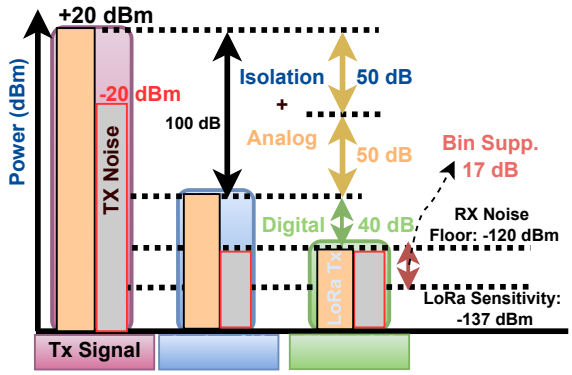

Figure 3: Self-Interference cancellation budget for LoRa. The requirement of analog cancellation (>100 dB) is much higher than in other applications such as WiFi. We must also cancel the residual SI 17 dB lower than the noise floor.

3 Requirements for LoRa Gateway Self Interference Cancellation

Self-interference cancellation (SIC) typically involves three stages [13, 24, 25] (Fig. 3): 1) Separation/Isolation between Tx-Rx antenna(e) 2) Analog Cancellation and 3) Digital Cancellation. The SIC requirements for the LoRa gateway stem from the unique features of LoRa communication and are different from full-duplex systems developed so far. Unlike short-range protocols (e.g., WiFi), LoRa supports long-range communication through a combination of features such as using lower frequencies (<920 MHz) and the ability to decode signals buried in noise. Therefore, designing a full duplex gateway for LoRa is challenging, as described below:

(i) Large analog cancellation: The transmission from a LoRa gateway comprises not only the main signal (LoRa Tx signal) but also broadband noise introduced by the transmitter, referred to as transmit noise (Tx noise), as shown in Fig. 3. Typical LoRa gateways transmit up to 20 dBm power. Our measurements of LoRa transmissions indicate the transmit noise to be at -20 dBm, 40 dB lower than the transmit power level. The SIC must remove both these components of self-interference (SI) to enable full duplex. The lowest possible noise floor of the LoRa gateway (corresponding to 125 kHz BW) is -120 dBm [26]. Therefore, we must cancel the Tx signal and Tx noise to -120 dBm. Thus, the full-duplex radio needs to achieve 140 dB (20-(-120)) cancellation for the SI arising from the Tx signal and 100 dB (-20-(-120)) cancellation for the SI due to Tx noise. Since digital cancellation cannot suppress Tx noise [13], there is a *requirement of at least 100 dB of analog cancellation.* This requirement is much higher than any previous full-duplex undertaking [27].

(ii) Cancellation over large delay spread: The SI is typically a superposition of several multipath reflections of the transmitted signal. Since each reflection arrives with a different delay, the cancellation circuit must re-create the superposition of the delayed reflections and cancel them. The time duration for which multipath reflections last – *delay spread* – has crucial implications on the design of the cancellation – specifically on analog cancellation. Since LoRa operates at a low 900 MHz band (3x lower than WiFi at 2.4 GHz), it can provide connectivity for longer distances (9x longer compared to 2.4 GHz WiFi) which leads to a large delay spread. *While traditional full duplex [13, 28, 29] can cancel only 5̃ ns delay spread, LoRa gateway must allow analog cancellation of up to 45 ns (9× longer) delay spread.*

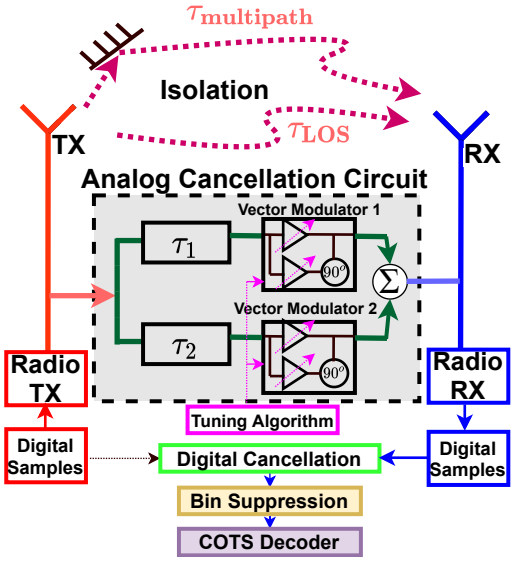

Figure 4: Full Duplex Cancellation Architecture with $\tau_1, \tau_2 < \tau_{LOS}, \tau_{multipath}$.

(iii) Cancellation below noise floor: Analog and digital cancellation combined can cancel the SI to the noise floor. Further SIC for LoRa is necessary and challenging since the decoder is sensitive well below the noise floor. To achieve long-range communication, LoRa uses chirp-spread-spectrum modulation to suppress wideband noise up to 17 dB below the thermal noise floor [26]. *Therefore, we must cancel SI 17 dB below the noise floor.*

4 LoRa Full Duplex Gateway Design

In this section, we present the design of the BSMA full-duplex LoRa gateway that enables in-band transmission of the Busy Signal while simultaneously receiving uplink packets. BSMA requires interference cancellation of the transmitted Busy Signal to decode the uplink packets. First, we describe the LoRa SI channel and its challenges in greater detail. Next, we present our cancellation design based on a novel analog short-delay approximation that can suppress the SI to the noise floor in conjunction with Digital cancellation. Finally, since the LoRA can decode signals below the noise floor – we design a cancellation in the de-chirped domain to eliminate residual SI such that there is a negligible impact on decoding the uplink packets, even below the noise floor.

4.1 LoRa SIC design: low bandwidth and high delay spread

The key challenge with designing SIC lies in achieving 100 dB of analog cancellation while handling high delay spread. SIC works by subtracting a synthesized copy of the interfering signal from the receiver path, which involves replicating the SI channel across the signal bandwidth using an analog/digital cancellation circuit. The high delay spread in the channel severely restricts the performance of state-of-the-art designs in LoRa, even though the bandwidth is low (125 kHz - 500 kHz).

4.1.1 *Single-tap cancellers will not work for LoRa*

The simplest solution is to use a single-tap frequency-flat canceller

such as [27], which emulates the SI channel using a single complex number (attenuation and phase). This method can reliably approximate the SI channel at a single frequency point, but not in channels with finite bandwidth and delay. Delays in the SI channel produce phase variation across the channel bandwidth, violating the frequency-flat assumption and limiting the cancellation achievable by a fixed-phase single-tap canceller [29]. The cancellation limit can be derived based on the channel bandwidth and the *delay-mismatch*, i.e., the difference between the channel's group delay and the single-tap canceller's group delay. Furthermore, practical wireless channels possess non-trivial, variable delay spread, leading to difficult gain/phase profiles and further performance degradation. Surprisingly, even for a channel bandwidth of 125 kHz, the cancellation is limited to ≈35 dB using a single-tap canceller with a delay-mismatch of 45 ns (Equation (1) from [29]). Frequency domain equalization techniques for 900 MHz [24] would also behave like single tap cancellers since the minimum frequency resolution for their operation is much larger than the LoRa bandwidth, calling for a method that better replicates the SI channel.

The general approach to replicating the delay in the SI channel is the time-domain approach [13, 25]. Figure 4 shows a tapped-delay line based analog cancellation architecture. In this design, the analog canceller takes a copy of the transmit signal, passes it through a fixed delay and variable attenuation, and subtracts it from the received signal to eliminate the SIC and Tx noise. The choice of fixed delays is close to the SI channel delay. The analog canceller needs to match the attenuation on each tapped delay to that of the self-interference channel and then eliminate the SI, similar to time-domain equalization. The tapped-delay line approach is ideal for our problem as its performance is practically unlimited so long as the delays and attenuation are chosen correctly.

4.1.2 Short Delay Approx. Analog Cancellation:

Directly adapting prior work on tapped-delay line cancellers to our application is difficult due to the larger delays in our SI channel. Long tap-delay lines are realized by laying out the physical length of a wire on a PCB. Such implementations incur a fixed loss per unit length: longer delays mean a higher signal loss on the canceller circuit and a significantly larger PCB area. The high signal loss reduces the maximum SI signal that can be canceled, reducing the dynamic range of the analog canceller.

Instead of designing extremely large and lossy PCBs to match the delay of the SI channel, we develop a technique to achieve high cancellation while keeping delays short. Our insight hinges on the observation that the SI channel is *almost frequency flat* within the short bandwidth. While a single frequency flat canceller will not achieve the required performance (>50 dB SIC), a combination of two cancellers with slightly different (short) delays can accurately reconstruct the SI. We can understand this by looking at how signals from two delay lines combine. Consider the complex baseband representation of the frequency domain channels $H_1(f), H_2(f)$ introduced by two separate delay lines in their complex baseband form: $H_1(f) = e^{-2\pi j f \tau_1}, H_2(f) = e^{-2\pi j f \tau_2}$. Where τ_1, τ_2 are the respective delays of each line, and f is the baseband frequency in Hz. Similarly the SI channel with a delay $\tau_{SI} (> \tau_1, \tau_2)$ can be written as $H_{SI}(f) = e^{-2\pi j f \tau_{SI}}$. Now, we write the resultant channel from the linear combination of the two delay lines as ($\alpha, \beta \in \mathbb{R}$ for simplicity):

$$\begin{aligned} \alpha H_1(f) + \beta H_2(f) &= \alpha e^{-2\pi j f \tau_1} + \beta e^{-2\pi j f \tau_2} \\ &\approx (\alpha + \beta) + \alpha(-2\pi j f \tau_1) + \beta(-2\pi j f \tau_2) \\ &\approx (\alpha + \beta) \exp(-2\pi j f \frac{\alpha\tau_1 + \beta\tau_2}{\alpha + \beta}) \\ &= (\alpha + \beta) \exp(-2\pi j f \tau_{net}) \end{aligned} \quad (1)$$

Where the first-order Taylor Series approximations are valid as long as $f\tau_1, f\tau_2 << 1$ for all f, which is equivalent to stating that the channel should have a *small time-bandwidth product*. While the SI channel has high delays, the bandwidth is small, yielding time-bandwidth products in the range of $(0, 0.006) << 1$ for a bandwidth of 125 kHz and 45 ns delay. By appropriately choosing the values of α, β (either could be negative), t_{net} could be made to mimic a range of t_{SI}. For example, choosing $\tau_1 = 8$ ns, $\tau_2 = 15$ ns, $\alpha = -0.5$, and $\beta = 1$ yields $\tau_{net} = 22$ ns. To the best of our knowledge, this is the first work that uses this phenomenon to approximate large delays. We can similarly derive a model for practical frequency domain channels where each channel has a complex multiplicative factor ($\alpha, \beta \in \mathbb{C}$). Furthermore, a superposition of N delays can be similarly expressed as a net delay using N Taylor Series expansions.

We collect extensive self-interference channel measurements using a Vector Network Analyzer (VNA) [30] at 100 locations in our deployment area to characterize the delay spread at 900 MHz. The VNA accurately measures the frequency response across its connected ports to 70 dB, clearly showing the component delays in the channel. Few power delay profile measurements are plotted in Figure 5(a) and show that delays as long as 45 ns exist in the 900 MHz SI channel.

To understand the efficacy of our technique, we perform a simulation where we evaluate the amount of cancellation achievable for an SI channel as we vary its group delay and bandwidth. We use a simulated analog cancellation PCB with two fixed taps (8 ns, 15 ns), each associated with a complex weight. The possible analog cancellation for each channel group delay and bandwidth is computed and plotted in Fig. 5(b). We make the following observations:

- At higher bandwidths (>1 MHz), the cancellation increases when the channel group delay matches the delays on the PCB but sharply drops when the two are different.
- At lower bandwidths (<1 MHz), the cancellation remains high for a much larger range of group-delay values, validating our claim that two shorter delays can approximate a longer one.

4.1.3 Designing the cancellation circuit:

Tx-Rx Antenna Isolation: Since our analog cancellation is expected to yield a cancellation of $\tilde{5}0$ dB from our simulations, the requirement for Tx-Rx antenna isolation is very high. While we can use new methods like Electrically Balanced Duplexers (EBD) to obtain high isolation, they are still an active area of research and not commercially available [31, 32]. We choose antenna separation[1] to provide the necessary isolation. We separate two dipole antennas vertically to minimize leakage and achieve >40 dB isolation at a separation of just 1 m [33, 34]. As a bonus, our short-delay approximation method is resilient to the additional delay in the SI channel due to the physical separation of the antennas.

[1] Antenna separation is feasible for fixed gateway deployments

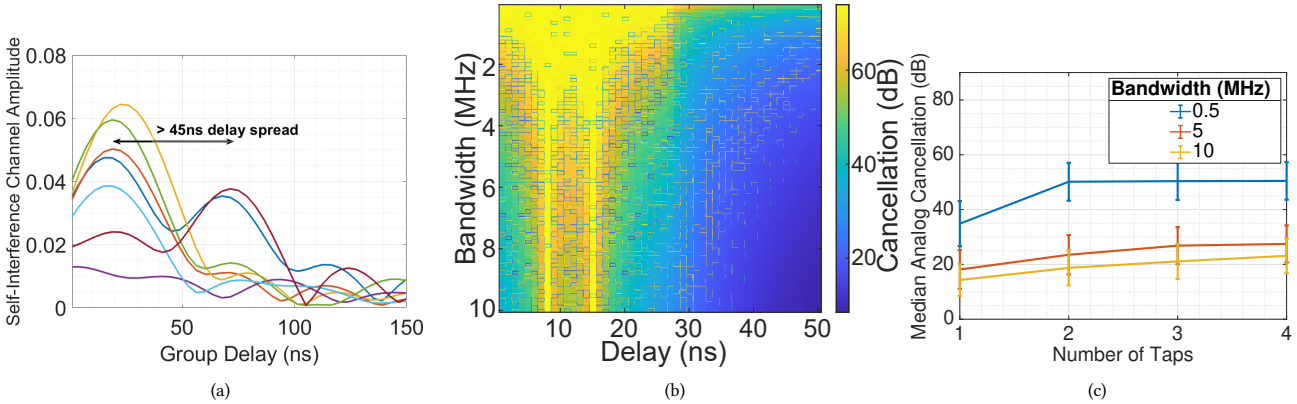

Figure 5: (a) Self Interference channel power-delay profile w.r.t group delay shows >45 ns delay spread among channels (b) SIC performance across delay and bandwidth; for small bandwidths, large delays can be approximated by smaller ones (c) SIC plotted against the number of taps and bandwidth: A single tap canceller will not work for LoRa, but two taps are enough.

Analog Cancellation: We use Vector Modulators (VMs) to provide complex weights on each tap-delay line, similar to [25]. To understand the number of tap-delay lines required in the canceller, we analyze the possible cancellation as the number of tap-delay lines increases. We use the SI channels from our VNA measurement study to perform this analysis and report projected cancellation for various channel bandwidths. Presented in Figure 5(c), we observe that a single-tap canceller does not provide the required cancellation as expected. Increasing the number of taps beyond two has diminishing returns on the improvement in cancellation. Real-life SI channels have multiple variable component delays, but due to the low delay-bandwidth product, these delays combine to approximate one net delay. Therefore, just two delay lines are required to meet the requirement of >50 dB analog cancellation. We perform a brute force search to obtain the best two delay values under 20 ns that maximize median cancellation across all the measured channels (8 ns and 15 ns). This search is justified since the design process for the analog canceller is a one-time undertaking. Once fabricated, it can be deployed and tuned in the field to maintain high cancellation, as discussed next.

Digital Cancellation: Since the analog SIC provides only 100 dB of cancellation, the additional 40 dB is taken care of post sampling in the digital domain. We borrow from the design in [13] and use the Least Squares method to estimate the FIR filter coefficients for linear and non-linear components of the transmit signal that best model the residual SI. We omit the details here for brevity and refer the reader to [13] for additional information.

Real-time tuning: As noted before, the analog cancellation consists of two tapped delay lines, each equipped with a vector modulator, i.e., complex weight attenuators. To continuously maintain SIC, we should constantly estimate the air channel between Tx & Rx and keep updating the weights of the complex attenuations. We leverage prior work [25] and its tuning algorithm and adapt it to work with our cancellation design.

4.2 Cancelling below noise floor with COTS

The LoRa decoder *de-chirps* the received signal and performs an FFT to demodulate data symbols, effectively combining the energy in the spread-spectrum signal. The residual SI consists of Tx noise and the Tx signal component, both at or below the noise power level at the receiver (Fig. 3).

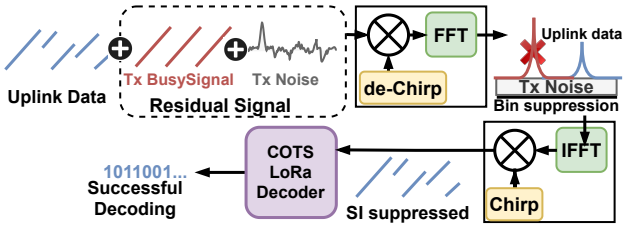

Figure 6: We cancel Busy Signal SI below the noise floor using the bin suppression technique. The de-chirp FFT allows us to extract the processing gain of the spread-spectrum modulation and identify the SI. We then remove the interference bin and re-modulate the signal with LoRa, allowing a COTS decoder to decode even low-SNR uplink data correctly.

The LoRa radio decoder is differently affected by the two components of residual SI. The spread-spectrum processing gain (up to 36 dB for SF12) suppresses the Tx noise due to its wideband nature. However, since the Busy Signal is also a LoRa modulated preamble to allow accurate CAD at all the devices, the residual Tx signal will enjoy the same processing gain after de-chirping. Residual Busy Signal interference is concentrated in one FFT bin, as shown in Fig. 6. A standard LoRa decoder may consistently mistake this interference for a symbol and declare wrong decisions.

We use a simple bin suppression technique post the FFT to leverage a COTS decoder, as shown in Fig. 6. This technique always suppresses the bin belonging to the Busy Signal, performs an IFFT, and hands over the samples to a COTS decoder after chirp modulation. While high SNR signals are unaffected by SI, low SNR signals can be detected and decoded only if the COTS decoder is not confused with a Busy Signal symbol. Consistently suppressing a bin causes the COTS decoder to be unable to decode that bin if it is present in the uplink data. The loss of one symbol from the entire alphabet (4096 for SF12) is insignificant and can be handled by LoRa physical layer channel coding; we were able to measure no performance degradation in decoding while using this method.

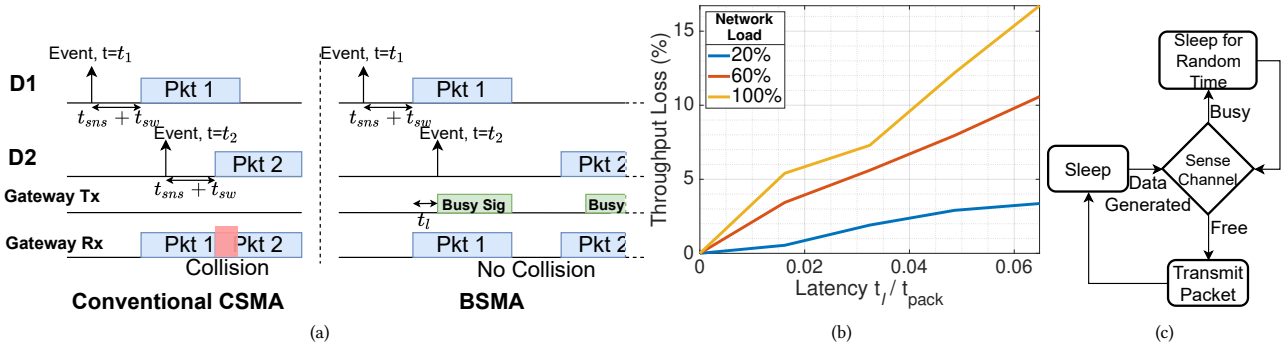

Figure 7: (a) A timing diagram illustrating the BSMA and the associated latencies. (b) Latency (as a function of packet size) in triggering the Busy Signal and the corresponding throughput loss at various network loads. (c) State diagram of non-persistent CSMA.

5 Busy Signal Multiple Access Design

As discussed in Section 2, CAD is ineffective in sensing ongoing uplink transmissions in urban environments, leading to 70% of hidden nodes in our deployment scenario and undermining the performance of CSMA. Since all the IoT devices are within range of the gateway, a Busy Signal transmission originating at the gateway can inform the entire network of the channel status and eliminate hidden nodes. Classic MAC protocols like [7, 9] implement similar busy signaling using sinusoidal tones at adjacent frequency bands. We take inspiration from these methods and build a signaling scheme that requires no modification to the IoT devices and functions with no channel overhead due to the full duplex gateway.

Anatomy of BSMA: Fig. 7(a) illustrates the operation of BSMA comparing it with conventional CAD-based CSMA. In both cases, COTS LoRa IoT devices wake up to transmit an uplink message in response to a sensory event. The IoT device first senses the channel using LoRa CAD for a duration of t_{sns} seconds. Upon detecting no ongoing transmissions, it switches from receive mode (necessary for sensing) to transmit mode in t_{sw} seconds and then transmits a packet for t_{pack} seconds. On the other hand, if CAD finds the channel busy, it defers its transmission for a later time.

In Fig. 7(a), two devices D1 and D2, hidden from each other, experience sensory events at times t_1 and $t_1 < t_2 < t_1 + T_{pack}$. In the case of CAD-based CSMA, D2, unable to sense D1 through CAD, initiates its transmission leading to a packet collision at the gateway. In the case of BSMA, the gateway detects the uplink packet from D1 and initiates a continuous downlink Busy Signal. As described later in this section, the Busy Signal comprises a sequence of LoRa preamble chirps. The Busy Signal exists for the entire duration of D1's packet. D2 detects the Busy Signal while performing CAD and defers its uplink transmission, thus avoiding the collision. This way, BSMA eliminates the hidden node problem.

Structure of the Busy Signal: COTS LoRa devices rely on detecting chirps for reliably performing CAD. Since the CAD module in LoRa reliably detects preamble-chirps within 1.5 symbol periods [26], it is the best candidate for the gateway initiated Busy Signal. To ensure that BSMA is compatible with CAD available in COTS LoRa devices, we use a sequence of LoRa chirps as the Busy Signal. Since interference from the Busy Signal can interfere with decoding uplink packets, the gateway must be full-duplex and cancel out the Busy Signal self-interference. As described in Section 1, without a full-duplex gateway, the Busy Signal would have to be transmitted over a separate channel and effectively halve the overall available bandwidth.

Flavors of CSMA at the IoT Devices CSMA comes in many flavors depending on how the IoT device defers transmission upon finding the channel busy. *p-persistent* CSMA is the most commonly used CSMA protocol, implemented in 802.11 WiFi systems [35]. Recent works have suggested similar persistent CSMA protocols for LoRa [4, 36]. However, persistent CSMA is designed to minimize channel idle time and therefore utilizes a lot of energy to sense the channel continuously. While this may be suitable for high-energy applications like WiFi, it is not suited for LPWANs like LoRa. In contrast, *non-persistent* CSMA is a protocol that defers its transmission by a random time if it instantaneously senses the channel to be busy. Since non-persistent CSMA does not "persist" in sensing the channel continuously, it improves energy efficiency by over 50% [37] while maintaining capacity. In this work, we use non-persistent CSMA in our deployments.

5.1 Effect of Busy Signal Latency

Ideally, the gateway must instantaneously detect and initiate the transmission of the Busy Signal. In practice however, the gateway incurs a non-zero latency to sense the uplink transmission and initiate a Busy Signal, deemed the Busy Signal latency, t_l in Fig. 7(a). In this section, we quantify the impact of Busy Signal latency on the performance of BSMA.

BSMA can be modeled as CSMA with no hidden nodes. The efficiency of CSMA has been extensively studied [11, 38]; we extend it to include the Busy Signal latency. In Fig. 7(a), if device D2 experiences an sensory event in the interval $t_1 < t_2 < t_1 + t_{sns} + t_{sw}$, it will not be able sense D1's transmission even if it is not a hidden node, since D1 only starts to transmit at $t_{sen} + t_{sw}$. Consequently, D2 will incorrectly assume the channel to be free and continue transmission, resulting in a packet collision. When the channel is experiencing a high utilization, the fraction $a = (t_{sns} + t_{sw}) / t_{pkt}$ fundamentally determines the probability of collisions and hence CSMA's efficiency [11][2]. Since BSMA incurs an additional latency of t_l before the Busy Signal is transmitted, the vulnerable period where D2 cannot sense D1 extends by an additional t_l seconds.

[2]The delays due to propagation time of light are negligible in this analysis.

Thus, BSMA's efficiency will be determined by:

$$a_{BSMA} = (t_l + t_{sns} + t_{sw})/t_{pkt} \quad (2)$$

In practice, $t_l \leq t_{sns}$ since the COTS gateway uses CAD to sense transmissions. In the absence of hidden nodes, BSMA's efficiency will be slightly lower than that of CSMA depending on t_l/t_{pkt}.

We relied on simulations to quantify the sensitivity of t_l/t_{pkt} on BSMA's performance. Fig. 7(b) depicts the loss in throughput in BSMA compared to CSMA without hidden nodes, as a function of t_l/t_{pkt} for three different traffic load conditions – low (20% of channel capacity), medium (60% of channel capacity) and high (100% channel capacity). In our simulations we used $t_{sns} = 3ms$ corresponding to SF8 at 125kHz bandwidth [26], $t_{sw} = 0.5ms$ based on measurements from our implementation and $t_{pkt} = 123.4ms$ based on 16 byte packets that we used in our deployment. As seen from Fig. 7(b), BSMA's throughput is significantly sensitive to t_l/t_{pkt}, especially at high traffic conditions; at t_l/t_{pkt} of 6% the throughput can drop as much as 15%. *Thus, the performance of BSMA is sensitive to t_l, and keeping it as low as possible is crucial to its efficient functioning.* Since t_l includes the time required by the COTS gateway to sense the uplink packet,$t_l > t_{sns}$. In our implementation, we achieve $t_l = 4.2$ ms including 3 ms of sensing delay. Thus, we operate at $t_l/t_{pkt} = 3\%$.

6 Implementation

To demonstrate the performance of BSMA and other MAC protocols, we identified the following requirements for testbed:

- Support practical outdoor deployments: Radius of deployment ≥ to a km. Should not rely on infrastructure/backhaul methods (like WiFi or LAN).
- Support many MAC protocols: After deployment, it is intractable to manually re-program each end device. Therefore, the end devices must be pre-programmed with a set of MAC protocols.
- Configuration and Backhaul: Device parameters should be remotely configurable. Statistics such as the number of packets sent and energy consumed should be backhauled wirelessly for performance evaluation.

We design the testbed to meet these requirements using COTS LoRa modules and a modified version of the popular open source *mcci-arduino-lmic* library [39] with inputs from [4]. We implement application layer functions in the Arduino platform that allow remote configuration and backhaul without recompiling. Since our code-base is Arduino compatible, it works with a wide variety of commonly used LoRa platforms such as [40, 41]. The codebase is available at **github.com/ucsdwcsng/bsma_lora**.

Gateway Implementation: Our gateway consists of a COTS LoRa decoder (SX1301 [42, 43]) augmented with a USRP-X300 Software Defined Radio (SDR) [44] and a custom analog SI canceller on a PCB. Shown in Fig. 8, **busy-signalling and analog cancellation are performed in real-time** by our SDR platform and the PCB canceller respectively. Due to hardware limitations on the FPGA, we perform digital cancellation and bin suppression in the host PC after receiving I/Q samples from the SDR platform. After the host completes full-duplex processing, the I/Q samples are re-transmitted to the SX1301-based gateway for full decoding, allowing throughput

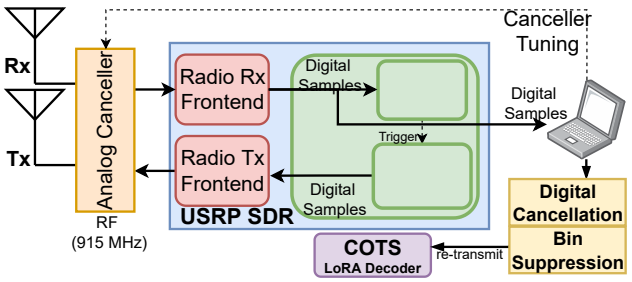

Figure 8: Full Duplex Gateway implementation showing all configuration and data paths. The reactive Busy Signal generator is implemented on the FPGA, a COTS decoder is used to decode packets. A host computer orchestrates all subsystems.

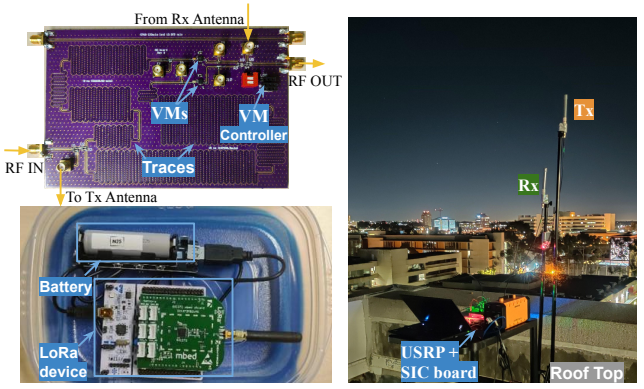

(a) (b)

Figure 9: Elements of the Testbed. (a) Top: The Full Duplex PCB featuring short-delay traces and vector modulators. Bottom: A battery-powered LoRa device in a box enclosure. (b) Rooftop gateway deployment. We deploy the devices outdoor on the university campus.

evaluation. We note here that commercial deployment of our solution can integrate the functions of BSMA as digital logic alongside the SX1301, similar to Section 3.9.2 described in [42]. The COTS gateway is also used to poll, configure, and retrieve data from the devices through a LoRa side channel.

Preamble detection at Gateway: We design preamble detection to minimize the FPGA resources used. LoRa preambles are composed of chirps whose frequency linearly increases with time [26]. We use auto-correlation, requiring only a single complex multiplication at sample rate regardless of the length of the sequence [45]. Auto-correlation is easier to implement in digital logic in comparison to match-filtering. We adjust the fixed point precision and threshold of the packet detector to achieve a TPR of 90% at -3 dB SINR with an FPR of 1%.

HDL and integration into SDR: We design a fixed point C++ implementation of the preamble detection algorithm considering input I/Q samples with 16 bits precision each, with double the precision (32 bits) for all internal computations. We design a busy signal generator that reads out stored preamble from BRAM whenever required. We use Vivado HLS to generate a Verilog HDL output for both blocks and incorporate it into the RFNoC 3 framework [46] compatible with the USRP. The parameters of each block, such as the energy threshold for the detector and the duty cycling for the busy signal generator, are exposed through GNURadio.

SI Cancellation Circuit: The full-duplex Analog Cancellation module sits before the gateway, providing self-interference cancellation. The cancellation circuit as shown in Fig. 9(a) is implemented on a PCB (10cm×15cm) using FR408-HR Isola [47] and using coplanar waveguides for delay lines. We use HMC630[48] Vector Modulators (VMs) which provide continuous gain control between [-50,-10] dB and 360^o phase control. I, Q pins of these VMs are driven by a 12-bit programmable DAC [49] controlled via I2C using an Arduino [50]. The busy signal transmitter block doubles as the Full-Duplex reference generator for tuning the analog and digital cancellation. To perform full-duplex training, we trigger this block manually. The cancellation requires only 15 symbol times to re-tune (≈30 ms), a negligible overhead. The gateway deployment showing antenna separation is in Fig. 9(b).

LoRa Devices: We use the SX1272 [19] shield along with a low-power STM32 microcontroller [51] for the devices (Fig. 9(a), bottom). The devices are battery-powered and not wired to a central controller. When required, device management and configuration occur through a LoRa side-channel. We can configure the devices to use different forms of CSMA or ALOHA as their MAC protocol. Parameters like generated load, size of packets, and experiment duration are configured wirelessly before each experiment. Upon receiving a broadcast beacon from the gateway, all devices involved in an experiment transmit uplink packets according to pre-set parameters. Once the experiment duration runs out, the devices transmit the results to the gateway through the LoRa side-channel.

7 Evaluation

Our goal with the evaluation is threefold: first, we present two case studies on the performance of BSMA over baseline MAC protocols on our hardware testbed. Second, using simulations, we show how BSMA's improvements on the hardware testbed will scale to thousands of devices and simultaneously optimize fairness, throughput, and energy consumption. Finally, we benchmark the achieved SI cancellation. The metrics used for evaluations are:

Throughput: Total network throughput at gateway.

Energy: Energy per Successful Packet.

Packet Reception Ratio (PRR): Total number of packets received without error, divided by the total number of packets transmitted.

Fairness: Represented using distributions of PRR.

Offered Load: The aggregate data traffic generated or *offered* by the devices to the network. It is expressed as a percentage of the maximum traffic the physical layer can support.

The key highlights of our evaluation are as follows:

- In outdoor hardware evaluations with 10 devices, evaluated over 5 days, with locations randomly sampled from Figure 2(a), BSMA provides 1.42x throughput improvement over CSMA, and 1.64x improvement over ALOHA.
- In bursty traffic conditions, BSMA's throughput is 2x better than CSMA due to its ability to virtually avoid most collisions. As an extension, the PRR and energy consumption are also 2x better for BSMA.
- The Full Duplex system is capable of 117.7 dB cancellation, of which 101.7 dB is in the analog domain. We show that our system provides 10x better cancellation over 250 kHz in comparison to a single-tap design.
- In a simulated environment with over 1000 devices, BSMA provides 1.75x throughput improvement over CSMA at 100% offered load.

Throughout the evaluations, the LoRa PHY parameters used are: SF8, 125 kHz, 4/8 Code Rate, Explicit Header mode with CRC, 16 Byte Packets (123.4 ms).

7.1 Case Study: Typical outdoor deployment

Experimental Setup: We randomly pick locations from our motivational experiment in Sec. 2 and deploy ten devices. The devices are static and mounted on light poles or trees roughly 6 ft from the ground. The gateway is on the rooftop of a tall building at an elevation of 25 m. The measured number of hidden nodes in this scenario is 77%. After deployment, the gateway configures each device to offer network traffic, as explained in the previous section. The configuration ensures that the aggregate network traffic is approximately Poisson with an average arrival rate equal to the configured network offered load. Depending on the experiment performed, the gateway configures the devices to use either ALOHA or CSMA. The CSMA experiments are repeated with and without BSMA's full-duplex capability. We use non-persistent CSMA with a sensing window of 2 CAD lengths, a unit backoff window of 12 ms, and max backoff of 64×12 ms for all our experiments. Each experiment lasts 100 seconds, and device indices and packet counters uniquely identify each packet.

Throughput: As expected, the throughput of the network increases with offered load (Fig. 10(a)). CSMA provides an average improvement of 1.2x over ALOHA, showing the expected performance from Fig. 2(d) is achieved due to the hidden nodes. BSMA alleviates the hidden node problem and achieves an average improvement of 1.4x over CSMA and 1.65x over ALOHA.

Packet Reception Ratio: PRR at 100% offered load is plotted for one day as a CDF across the 10 devices to visualize the network's ability to maintain fairness. Since each device offers the same number of packets to the network on average, the PRR performance across all devices should be the same to maintain fairness. From Fig. 10(b), we see that ALOHA and CSMA fail to support more than 0.6 PRR for any of the devices. However, the introduction of BSMA improves the median PRR by 0.18, with a maximum increase of 0.38. BSMA's MAC functions to enhance the performance of all devices near and far. The spread of BSMA's CDF in Fig. 10(b) is due to unavoidable residual collisions, where one or more may get decoded due to the capture effect.

Energy Consumption: In Fig.10(c), we compute the average amount of energy used by the network per successful packet by estimating the amount of energy used by every device (due to channel sensing and actual packet transmission) and dividing it by the total number of packets successfully decoded at the gateway. We use the power measurements from [4] to compute the metrics. In the case of ALOHA, there is no energy spent on channel sensing, but the energy consumed is the largest. Packet collisions are high in ALOHA, and collisions lead to wasted energy (since the gateway may not correctly decode one or more of the packets involved). In contrast, energy consumption in CSMA is lower due to minimal collision avoidance among the few devices that are not hidden. BSMA's energy consumption is the lowest since it minimizes collisions and

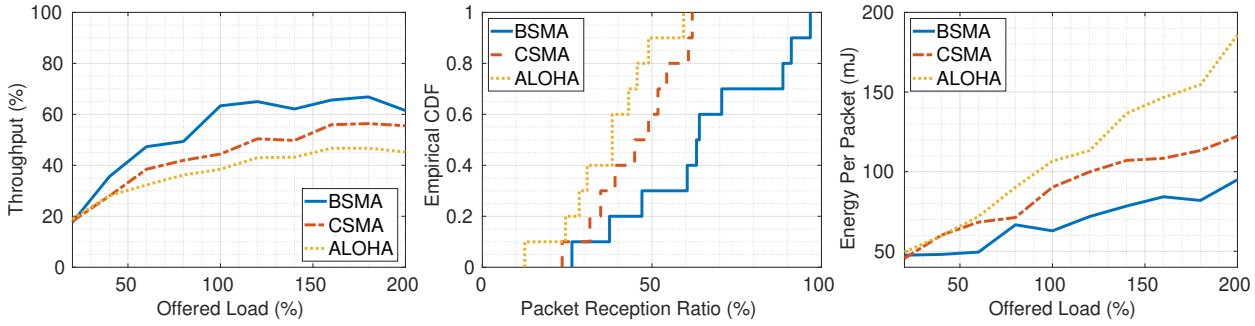

(a) (b) (c)

Figure 10: (a). Throughput improvement of BSMA over conventional MAC protocols in an outdoor deployment. (b) BSMA improves PRR performance across all devices as it reduces collisions, (c) Due to higher throughput and the use of non-persistent CSMA, the energy consumption of BSMA is reduced.

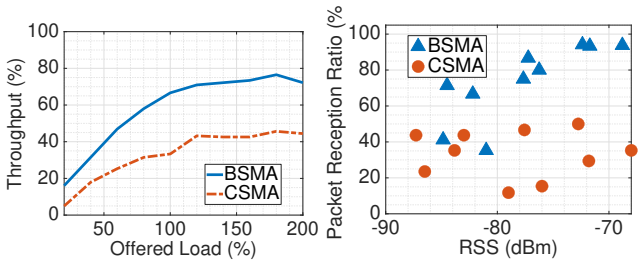

(a) (b)

Figure 11: (a). Throughput performance of BSMA with bursty traffic. (b) The scatter plot of receive power at the gateway w.r.t the PRR shows that BSMA improves PRR for all devices.

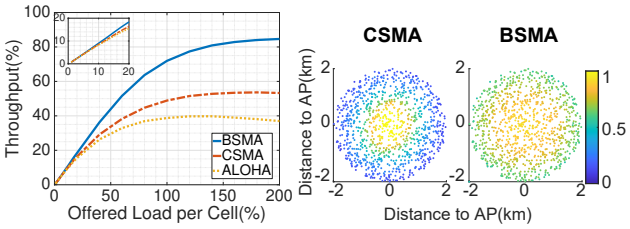

(a) (b)

Figure 12: Thousand device simulations: (a) throughput performance (b) PRR distribution w.r.t device location. Each dot is a device, and its PRR is encoded in the color (brighter the better). BSMA therefore improves throughput while maintaining fairness.

improves throughput. On average BSMA's energy consumption is 1.3× better than CSMA and 1.8× better than ALOHA.

7.2 Case Study: Bursty traffic

Experimental Setup: In commercial LoRa deployments, traffic is sometimes periodic and bursty due to duty-cycling restrictions and periodic sensor readings [52, 53]. We create periodic traffic by modifying the offered load pattern and having each device generate packets at a fixed period with a random uncertainty of 10 ms. As the offered load increases, the mean length of the period is decreased. CSMA and BSMA are evaluated in this study.

Throughput: Due to the bursty nature of the traffic, the probability of collisions is much higher when hidden nodes are present, leading to poor performance with CSMA. In Fig 11(a), we see that BSMA is 2x better than CSMA beyond 100% load.

Packet Reception Ratio: The PRR performance across devices at a particular load shows how BSMA improves fairness. In Fig. 11(b), we see that BSMA improves PRR for all devices, regardless of their received power at the gateway, with a median gain of 2x. The energy consumption metric also follows the same trend, with BSMA providing a 2x reduction per packet.

7.3 Scaling LPWANs to thousands of devices

Simulation Framework: We use simulations to evaluate the performance of BSMA in larger-scale settings. We implement a custom simulation framework in MATLAB that allows arbitrary gateway/device placements, multiple MAC protocols at the devices (CSMA, ALOHA), gateway busy-signaling, and models capture effect. Existing LoRa simulators do not model capture effect or hidden links [3, 54]. LoRa physical layer parameters are configurable, and packet error rate thresholds described in [26] are used to model decoding. We implement capture effect based on the SINR threshold models from [6, 53, 55]. Two devices are considered to be hidden w.r.t each other if the distance between them is greater than 660 m, chosen based on our observations from Section 2.

Experimental Setup: We perform a simulation to evaluate the capability of BSMA to handle thousands of devices like in large-scale sensor networks. We deploy 1000 devices in a 2 km radius around a single gateway. All devices can communicate with the gateway and vice-versa, but the hearing range for CAD is set according to the LDPL model discussed in Section 2. We evaluate Throughput, PRR, and Fairness against various offered loads. We perform the simulation for BSMA, CSMA, and ALOHA. Since we solve the hidden node problem, we see a higher throughput for the same amount of offered load. The improvement over conventional CSMA approaches 1.8x at 100% offered load (Fig. 12(a)). We also evaluate the performance of BSMA when the aggregate offered load is low (1-20%). In these low-load, low-collision scenarios, the performance improvement of BSMA over CSMA and ALOHA increases with offered load, being 1.1x better than CSMA at 17.5% load. Although BSMA's performance gains are low in the low-load cases, it is always marginally better than CSMA and ALOHA.

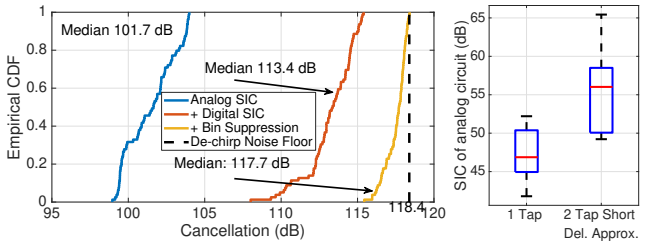

(a) (b)

Figure 13: (a) CDF of BSMA's SIC over 10 seconds, split into component stages. Analog SIC provides a median cancellation > 100 dB. Digital cancellation provides additional 12 dB, and finally, bin suppression takes SI to the instrument noise floor. We measure median noise floor degradation of 0.7 dB in the de-chirped domain since the residual SI leaks to some adjacent bins. (b) Analog cancellation performance across 7 locations using a single tap vs our two tap (short delay approximation). Only our two tap approach consistently meets the cancellation budget.

PRR Distribution and Fairness: Fairness in each of these MAC protocols is affected by the number of collisions and capture effect. Even with significant SNR variations between devices, BSMA can enforce fairness and allow all devices to transmit comparable packets. In Fig. 12(b), we visualize the network deployment in 2-D, where each device is a point. The colors correspond to the PRR per device. For ALOHA and CSMA, devices closer to the gateway enjoy better PRR than those farther away. Neither of the baseline MAC protocols can curb packet collisions, leading to capture effect and consistent decoding of high-power packets (i.e., from devices closer to the gateway). By controlling collisions, BSMA can provide equitable PRR across the entire deployment.

7.4 Full Duplex Cancellation Study

In Fig. 13(a), we present the total cancellation of our Full Duplex SIC technique over 10 seconds. We split the performance into component stages: Analog cancellation provides >100 dB (45.5 dB from antenna isolation, 56.2 dB from the analog circuit), and the SI is taken to the noise floor by digital cancellation and bin suppression. Even with the processing gain of chirp-spread-spectrum, the noise floor measured is much higher than thermal noise due to hardware limitations on the USRP. In addition, the Tx chain of the USRP has a P1dB of around 10 dBm, preventing us from transmitting higher signal power. These effects limit the observable cancellation to a median of 117.7 dB. Since our technique always cancels SIC to the noise floor after de-chirping, we expect it to perform better with commercial LoRa baseband processors designed with better noise and linearity performance [42].

7.4.1 Benchmark: single tap vs Short delay approx.: In Fig. 13(b), we evaluate the effectiveness of the short-delay approximation method using two taps compared to using only a single tap for cancellation. By switching off one of the VMs in our PCB, we can perform cancellation with a single tap, similar to approaches like [24, 27]. The cancellation is evaluated over the channels presented in Figure 5(a). Even though the bandwidth for LoRa uplink is small (<250 kHz) in comparison to conventional full duplex applications, the large delay spread prevents a single tap gain/phase control from providing the necessary (> 50 dB) analog cancellation.

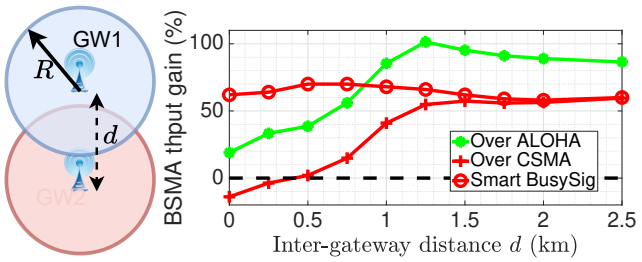

(a) (b)

Figure 14: BSMA and multi-network deployments. (a) Illustration of a two network deployment overlapping cells of the same radius (R = 1 km). The cells also denote each gateway's busy-signal range. The inter-gateway distance d is varied for the simulation study. (b) BSMA's aggregate throughput (across both networks) gain as a function of d for an offered load of 100% per cell.

In contrast, our 2-tap method is 10dB (10×) better in the median and achieves the target cancellation budget.

8 Discussion and Future work

Multi-gateway deployments: Typical city-wide LoRa deployments use multiple gateways [18]. Carrier sense-based multiple access protocols could lead to exposed node problems in such deployments [9]. While a single network operator could deploy cells to minimize the exposed nodes, LoRa cells run by independent entities could overlap and cannot be co-designed. Therefore, we evaluate a multi-gateway BSMA scenario in simulation.

Consider two co-channel (same frequency, SF) LoRa gateways (GW1 & GW2) belonging to independent networks with overlapping cells as shown in Fig. 14(a), where the cell radius is R (=1 km), and inter-gateway distance is d. Each network has 100 randomly placed devices in its cells. Devices offer the same aggregate traffic to their respective networks. Other simulation parameters are the same as Section 7.3. By design, the busy signal from each gateway would be heard by all devices within its cell. Since this includes some devices from the other network, it contributes to the exposed node problem. In addition, the busy signal from GW1 could degrade the SINR at GW2 (and vice-versa) if the gateways themselves are within each other's cells.

The performance of BSMA in comparison to ALOHA and CSMA as a function of inter-gateway distance d is presented in Figure 14(b). BSMA always performs better than ALOHA but becomes worse than CSMA when the gateways are closer than 500 m due to busy-signal SINR degradation. We can counter the inter-gateway busy-signal interference by transmitting just enough power in the busy signal to reach the device (say A) that triggered it. Through this, all devices closer (and therefore having higher SNR at the gateway) than device A will not interfere with the transmission of device A. Devices that have lower SNR at the gateway than device A will not interfere due to the capture effect, safeguarding throughput. Also, the predictable nature of the busy signal interference allows canceling schemes such as [56, 57] can be used to reduce inter-gateway interference further. The curve "Smart BusySig" in Fig. 14(b) illustrates the potential gain when inter-gateway interference is completely avoided. The "Smart BusySig" curve is flat with d, indicating that performance is minimally affected by the exposed node problem. Upon deeper analysis, we concluded that

the exposed nodes in such deployments lead to received signal strengths at both gateways in a range that causes packet loss due to collision (i.e., the gateway decodes the packet from the wrong network). We leave a detailed study of these ideas for future work.

BSMA deployment considerations: BSMA reduces packet collisions and is most useful in deployment scenarios where instantaneous offered load could be high (>20%). As described in this work, a single gateway deployment serving many end devices is the best candidate for the system. The gains of using BSMA are diminished in LoRa due to extreme capture effect [53]. BSMA would perform even better in cases where capture effect is reduced, like when LoRa preambles collide [6] or in other IoT protocols.

Costs of deploying BSMA: BSMA's major strength is that it requires no modification to COTS end-devices. Implementing full-duplex function at the gateway alone is feasible with COTS systems (described in Sec. 6), requires minimal tuning overhead (30 ms, Sec. 4), and provides stable SIC commensurate to the application requirements (>100 dB, Sec. 7.4). The energy overhead of transmitting a busy signal occurs only at the gateway and is acceptable since the gateway is not power constrained in most deployments.

9 Related Work

The cross-layer nature of this work is related to a large body of work across the PHY and MAC domains, as summarized below.

Full Duplex Radio: Self interference suppression is done using a combination of isolation, analog cancellation and digital cancellation [13, 15, 16, 24, 25, 58–61]. Isolation techniques use antenna separation [58–61], circulators [13, 24, 25, 62, 63], or hybrid junction based methods [27, 31, 32] to implement the first stage of isolation between the receiver and the transmitter. Hybrid junction-based isolation techniques use couplers [27, 32] or Electrical-Balanced Duplexers (EBDs) [31] with a tunable impedance and are typically employed in continuous wave (CW) transmit signal systems. CW transmit signals are used backscatter systems like RFID [64–66], and more recently in LoRa backscatter [27]. While these techniques can provide over 75 dB of isolation for a CW signal [27], they do not extend even to narrow-band signals. Tuned Hybrid junctions will behave as single-tap cancellers and cannot match the delay-spread induced phase profile over the entire bandwidth, and cannot exclusively provide the required 100 dB of analog cancellation (Section 4.1). Magnetic [13, 24, 25] and small form factor integrated circulators [62, 63] have been developed, but are limited in their isolation capability to under 30 dB (magnetic), and 40 dB (integrated) in typical narrow-band antenna terminated applications [63, 67]. BSMA's choice of using antenna separation provides uniform isolation across the narrow-band channel. The antenna separation (75 cm) required for the >45 dB isolation is feasible due to the fixed nature of gateways and their form factor.

Analog cancellation circuits augment cancellation provided by isolation techniques using a tap-delay line [13, 15, 25] or frequency domain cancellation [24] methods. Tap delay-line approaches use delays as large as those in the SI channel. In our case, these delays are too large to lay out on a PCB. [24] work in the frequency domain but are equivalent to a single tap for our bandwidth of interest (125 kHz) and achieve only 52 dB of analog SIC (including 20 dB from isolation). None of these approaches have achieved > 100 dB of analog cancellation in conjunction with isolation [27]. In addition to 45 dB of isolation, our short-delay approximation-based analog canceller can provide an additional 56 dB of SIC.

Digital cancellation techniques can further cancel the residual signal to the noise floor or below it [13, 24]. BSMA builds on prior digital cancellation methods and implements a busy-signal aware bin-suppression. By taking advantage of the known signal properties of the busy signal and the chirp processing gain of LoRa, canceling SI to well below the noise floor is feasible.

Out of Band Busy Signalling: Using out-of-band busy signaling in CSMA to alleviate the hidden node problem is well studied [7–10]. These techniques require additional frequency resources and are generally considered unreliable due to the narrow-band nature of the Busy Signal sine-tone [11, 12]. This work eliminates the overhead and specifically designs the BSMA solution for LoRa. To the best of our knowledge, no prior work has evaluated Busy Signal with full duplex.

MAC for LoRa: There has been significant interest in improving the LoRa MAC beyond the default ALOHA. [68–70] propose time synchronisation for slotted medium access. But these methods increase overhead and power consumption on the devices. [4] proposes, in part, the use of persistent CSMA over ALOHA but does not address the hidden node problem in its outdoor deployments. [4] further proposes frequency and code-domain hopping to improve CSMA performance. In contrast, BSMA focuses on improving performance within a single channel. The hopping ideas from [4] can be incorporated into BSMA to improve performance further. [5, 36, 55] suggest using RTS/CTS based mechanism to resolve the hidden node problem. RTS/CTS messages are comparable in size to LoRa packets (typically only a few bytes) and cause high overhead (up to 200%).

LoRa Concurrent Decoding: Recently several researchers have focused on developing a robust LoRa PHY decoder to alleviate the high rate of collisions using concurrent decoding [71–76]. Our work complements these techniques by developing a no-overhead method to control collisions. Analysis in [2, 74, 75] indicates that no more than 5-10 transmissions be decoded simultaneously. We envision a system where busy-signaling can be used to block the channel exactly when the maximum number of simultaneous collisions happen, *i.e.* the system deliberately allows collisions to the extent to which concurrent decoding can be applied to achieve improvement. BSMA is not limited to the LoRa and can work with any protocol that supports channel sensing at the devices.

10 Acknowledgements

We thank the anonymous reviewers and the shepherd for their insightful comments, suggestions, and help in improving this work. We thank Howard Chi, Roshan Ayyalasomayajula, Agrim Gupta, and other members of WCSNG at UCSD for their help and feedback with the evaluations.

References

[1] Semtech. What is LoRa? https://www.semtech.com/lora/what-is-lora. Retrieved February 26, 2021.

[2] Branden Ghena, Joshua Adkins, Longfei Shangguan, Kyle Jamieson, Philip Levis, and Prabal Dutta. Challenge: Unlicensed lpwans are not yet the path to ubiquitous connectivity. In *The 25th Annual International Conference on Mobile Computing and Networking*, pages 1–12, 2019.

[3] Martin C Bor, Utz Roedig, Thiemo Voigt, and Juan M Alonso. Do lora low-power wide-area networks scale? In *Proceedings of the 19th ACM International Conference on Modeling, Analysis and Simulation of Wireless and Mobile Systems*, pages 59–67, 2016.

[4] Amalinda Gamage, Jansen Christian Liando, Chaojie Gu, Rui Tan, and Mo Li. Lmac: Efficient carrier-sense multiple access for lora. In *Proceedings of the 26th Annual International Conference on Mobile Computing and Networking*, MobiCom '20, New York, NY, USA, 2020. Association for Computing Machinery.

[5] Morgan O'kennedy, Thomas Niesler, Riaan Wolhuter, and Nathalie Mitton. Practical evaluation of carrier sensing for a lora wildlife monitoring network. In *2020 IFIP Networking Conference (Networking)*, pages 614–618. IEEE, 2020.

[6] Jansen C. Liando, Amalinda Gamage, Agustinus W. Tengourtius, and Mo Li. Known and unknown facts of lora: Experiences from a large-scale measurement study. *ACM Trans. Sen. Netw.*, 15(2), February 2019.

[7] F. Tobagi and L. Kleinrock. Packet switching in radio channels: Part ii - the hidden terminal problem in carrier sense multiple-access and the busy-tone solution. *IEEE Transactions on Communications*, 23(12):1417–1433, 1975.

[8] Cheng-shong Wu and V Li. Receiver-initiated busy-tone multiple access in packet radio networks. In *Proceedings of the ACM workshop on Frontiers in computer communications technology*, pages 336–342, 1987.

[9] Z. J. Haas and Jing Deng. Dual busy tone multiple access (dbtma)-a multiple access control scheme for ad hoc networks. *IEEE Transactions on Communications*, 50(6):975–985, 2002.

[10] Hong-Ning Dai, Kam-Wing Ng, and Min-You Wu. A busy-tone based mac scheme for wireless ad hoc networks using directional antennas. In *IEEE GLOBECOM 2007-IEEE Global Telecommunications Conference*, pages 4969–4973. IEEE, 2007.

[11] Paulette Altmaier. A Short Tutorial on CSMA: IEEE P802.11191-44-A . https://www.ieee802.org/11/Documents/DocumentArchives/1991_docs/1191044A_scan.pdf, 1991. Retrieved January 26, 2021.

[12] Chandos A. Rypinski. COMMENTS ON -A SHORT TUTORIAL ON CSMA-(IEEE P802.11/91-44) . https://www.ieee802.org/11/Documents/DocumentArchives/1991_docs/1191056_scan.pdf, 1991. Retrieved January 26, 2021.

[13] Dinesh Bharadia, Emily McMilin, and Sachin Katti. Full duplex radios. In *Proceedings of the ACM SIGCOMM 2013 conference on SIGCOMM*, pages 375–386, 2013.

[14] Yang-Seok Choi and Hooman Shirani-Mehr. Simultaneous transmission and reception: Algorithm, design and system level performance. *IEEE Transactions on Wireless Communications*, 12(12):5992–6010, 2013.

[15] Dinesh Bharadia and Sachin Katti. Full duplex {MIMO} radios. In *11th {USENIX} Symposium on Networked Systems Design and Implementation ({NSDI} 14)*, pages 359–372, 2014.

[16] J. Tamminen, M. Turunen, D. Korpi, T. Huusari, Y. Choi, S. Talwar, and M. Valkama. Digitally-controlled rf self-interference canceller for full-duplex radios. In *2016 24th European Signal Processing Conference (EUSIPCO)*, pages 783–787, 2016.

[17] ALOHA. Standard MAC Protocol. https://en.wikipedia.org/wiki/ALOHAnet. Retrieved March 10, 2021.

[18] LoRa Alliance. What is LoRaWAN Specification. https://lora-alliance.org/about-lorawan/. Retrieved February 26, 2021.

[19] Semtech. Semtech SX1272MB2DAS, LoRa Core™ Mbed Shield, SX1272, 868 and 915MHz. https://www.semtech.com/products/wireless-rf/lora-transceivers/sx1272mb2das. Retrieved February 26, 2021.

[20] Salaheddin Hosseinzadeh (2021). PYTHON/MATLAB optimization for log-distance model + Example. https://www.mathworks.com/matlabcentral/fileexchange/70097-python-matlab-optimization-for-log-distance-model-example. Retrieved January 26, 2021.

[21] Dhananjay Jagtap, Alex Yen, Huanlei Wu, Aaron Schulman, and Pat Pannuto. Federated infrastructure: Usage, patterns, and insights from "the people's network". In *Proceedings of the 21st ACM Internet Measurement Conference*, IMC '21, page 22–36, New York, NY, USA, 2021. Association for Computing Machinery.

[22] Jeongkeun Lee, Wonho Kim, Sung-Ju Lee, Daehyung Jo, Jiho Ryu, Taekyoung Kwon, and Yanghee Choi. An experimental study on the capture effect in 802.11a networks. In *Proceedings of the Second ACM International Workshop on Wireless Network Testbeds, Experimental Evaluation and Characterization*, WinTECH '07, page 19–26, New York, NY, USA, 2007. Association for Computing Machinery.

[23] C. Ware, J. Chicharo, and T. Wysocki. Simulation of capture behaviour in ieee 802.11 radio modems. In *IEEE 54th Vehicular Technology Conference. VTC Fall 2001. Proceedings (Cat. No.01CH37211)*, volume 3, pages 1393–1397 vol.3, 2001.

[24] Tingjun Chen, Mahmood Baraani Dastjerdi, Jin Zhou, Harish Krishnaswamy, and Gil Zussman. Wideband full-duplex wireless via frequency-domain equalization: Design and experimentation. In *The 25th Annual International Conference on Mobile Computing and Networking*, pages 1–16, 2019.

[25] Dani Korpi, Joose Tamminen, Matias Turunen, Timo Huusari, Yang-Seok Choi, Lauri Anttila, Shilpa Talwar, and Mikko Valkama. Full-duplex mobile device: Pushing the limits. *IEEE Communications Magazine*, 54(9):80–87, 2016.

[26] Semtech. Semtech SX1272, Long Range, Low Power RF Transceiver 860-1000 MHz with LoRa Technology. https://www.semtech.com/products/wireless-rf/lora-transceivers/sx1272. Retrieved February 26, 2021.

[27] Mohamad Katanbaf, Anthony Weinand, and Vamsi Talla. Simplifying backscatter deployment: Full-duplex lora backscatter. In *18th {USENIX} Symposium on Networked Systems Design and Implementation ({NSDI} 21)*, pages 955–972, 2021.

[28] Aravind Nagulu, Sasank Garikapati, Mostafa Essawy, Igor Kadota, Tingjun Chen, Arun Natarajan, Gil Zussman, and Harish Krishnaswamy. 6.6 full-duplex receiver with wideband multi-domain fir cancellation based on stacked-capacitor, n-path switched-capacitor delay lines achieving >54db sic across 80mhz bw and >15dbm tx power-handling. In *2021 IEEE International Solid- State Circuits Conference (ISSCC)*, volume 64, pages 100–102, 2021.

[29] Dirk-Jan van den Broek, Eric AM Klumperink, and Bram Nauta. An in-band full-duplex radio receiver with a passive vector modulator downmixer for self-interference cancellation. *IEEE journal of solid-state circuits*, 50(12):3003–3014, 2015.

[30] Keysight. Vector Netowrk Analyser. https://www.keysight.com/en/pdx-x201873-pn-E5072A/ena-vector-network-analyzer?cc=US&lc=eng. Retrieved March 10, 2021.

[31] Barend van Liempd, Benjamin Hershberg, Saneaki Ariumi, Kuba Raczkowski, Karl-Frederik Bink, Udo Karthaus, Ewout Martens, Piet Wambacq, and Jan Craninckx. A +70-dbm iip3 electrical-balance duplexer for highly integrated tunable front-ends. *IEEE Transactions on Microwave Theory and Techniques*, 64(12):4274–4286, 2016.

[32] Kun-Da Chu, Mohamad Katanbaf, Tong Zhang, Chenxin Su, and Jacques C. Rudell. A broadband and deep-tx self-interference cancellation technique for full-duplex and frequency-domain-duplex transceiver applications. In *2018 IEEE International Solid - State Circuits Conference - (ISSCC)*, pages 170–172, 2018.

[33] COMMSCOPE. Antenna Vertical Isolation Calculator. https://extapps.commscope.com/calculators/qvisolation.aspx. Retrieved March 4, 2021.

[34] NSW Government Telco Authority. Antenna Placement and Isolation Guideline. https://www.telco.nsw.gov.au/sites/default/files/4-3-2-001%20Antenna%20Placement%20Guideline%20v1.0.pdf. Retrieved March 4, 2021.

[35] R. Bruno, M. Conti, and E. Gregori. Optimization of efficiency and energy consumption in p-persistent csma-based wireless lans. *IEEE Transactions on Mobile Computing*, 1(1):10–31, 2002.

[36] Congduc Pham and Muhammad Ehsan. Dense deployment of lora networks: Expectations and limits of channel activity detection and capture effect for radio channel access. *Sensors*, 21(3):825, 2021.

[37] Douglas S Chan, Toby Berger, and Raj Bridgelall. Energy efficiency of csma protocols for wireless packet switched networks. In *2004 IEEE Wireless Communications and Networking Conference (IEEE Cat. No. 04TH8733)*, volume 1, pages 447–452. IEEE, 2004.

[38] Leonard Kleinrock and Fouad Tobagi. Packet switching in radio channels: Part i-carrier sense multiple-access modes and their throughput-delay characteristics. *IEEE transactions on Communications*, 23(12):1400–1416, 1975.

[39] MCCI. Arduino-LMIC library. https://github.com/mcci-catena/arduino-lmic. Retrieved March 10, 2021.

[40] HOPERF. LoRAWAN Module. https://www.hoperf.com/modules/LoRaWAN/RFM6501W.html. Retrieved March 10, 2021.

[41] MCCI. MCCI Catena for LoRAWAN Technology. https://store.mcci.com/products/mcci-catena-4610-integrated-node-for-lorawan-technology. Retrieved March 10, 2021.

[42] Semtech. Semtech SX1301, LoRa Core Digital Baseband Chip for outdoor LoRaWAN network macro gateways. https://www.semtech.com/products/wireless-rf/lora-gateways/sx1301.

[43] RAK. RAK2245 RPi HAT Edition, WisLink LPWAN Concentrator. https://store.rakwireless.com/products/rak2245-pi-hat. Retrieved March 10, 2021.

[44] Ettus Research. USRP X300. https://www.ettus.com/all-products/x300-kit/. Retrieved February 26, 2022.

[45] Schmidl & Cox. Algorithm for Preamble Detection. https://dspillustrations.com/pages/posts/misc/schmidlcox-synchronization-for-ofdm.html. Retrieved March 10, 2021.

[46] Ettus Research. RF Network on Chip. https://www.ettus.com/sdr-software/rfnoc/. Retrieved March 10, 2021.

[47] ISOLA Group. high-performance FR-4 resin system with a 230 C (DMA) Tg for multilayer PCB applications. https://www.isola-group.com/pcb-laminates-prepreg/fr408hr/. Retrieved March 4, 2021.

[48] Analog Devices. Vector Modulator for 700-1000 MHz frequencies. https://www.analog.com/media/en/technical-documentation/data-sheets/hmc630.pdf. Retrieved March 4, 2021.

[49] Micro Chip. 12-bit Quad Digital-to-Analog Converter with EEPROM Memory. https://ww1.microchip.com/downloads/en/DeviceDoc/22187E.pdf. Retrieved March 4, 2021.

[50] Arduino. 32-bit ARM core microcontroller. https://store.arduino.cc/usa/due. Retrieved March 4, 2021.

[51] ST Microelectronics. NUCLEO-L073RZ: STM32 Nucleo-64 development board with STM32L073RZ MCU. https://www.st.com/en/evaluation-tools/nucleo-l073rz.html. Retrieved February 26, 2021.

[52] TU Delft. RoN 2017 Report on IoT. https://wiki.surfnet.nl/display/SURFnetnetwerkWiki/.

[53] Andri Rahmadhani and Fernando Kuipers. When lorawan frames collide. In *Proceedings of the 12th International Workshop on Wireless Network Testbeds, Experimental Evaluation & Characterization*, pages 89–97, 2018.

[54] T. To and A. Duda. Simulation of lora in ns-3: Improving lora performance with csma. In *2018 IEEE International Conference on Communications (ICC)*, pages 1–7, 2018.

[55] Jetmir Haxhibeqiri, Floris Van den Abeele, Ingrid Moerman, and Jeroen Hoebeke. Lora scalability: A simulation model based on interference measurements. *Sensors*, 17(6):1193, 2017.

[56] Yaxiong Xie, Jie Xiong, Mo Li, and Kyle Jamieson. md-track: Leveraging multi-dimensionality for passive indoor wi-fi tracking. In *The 25th Annual International Conference on Mobile Computing and Networking*, pages 1–16, 2019.

[57] Pulin Patel and Jack Holtzman. Analysis of a simple successive interference cancellation scheme in a ds/cdma system. *IEEE journal on selected areas in communications*, 12(5):796–807, 1994.

[58] Tolga Dinc and Harish Krishnaswamy. At/r antenna pair with polarization-based reconfigurable wideband self-interference cancellation for simultaneous transmit and receive. In *2015 IEEE MTT-S International Microwave Symposium*, pages 1–4. IEEE, 2015.

[59] Melissa Duarte, Ashutosh Sabharwal, Vaneet Aggarwal, Rittwik Jana, KK Ramakrishnan, Christopher W Rice, and NK Shankaranarayanan. Design and characterization of a full-duplex multiantenna system for wifi networks. *IEEE Transactions on Vehicular Technology*, 63(3):1160–1177, 2013.

[60] A. Kumar and S. Aniruddhan. A 2.35 ghz cross-talk canceller for 2x2 mimo full-duplex wireless system. In *2019 IEEE MTT-S International Microwave Symposium (IMS)*, pages 877–880, 2019.

[61] Evan Everett, Achaleshwar Sahai, and Ashutosh Sabharwal. Passive self-interference suppression for full-duplex infrastructure nodes. *IEEE Transactions on Wireless Communications*, 13(2):680–694, 2014.

[62] Negar Reiskarimian, Mahmood Baraani Dastjerdi, Jin Zhou, and Harish Krishnaswamy. Analysis and design of commutation-based circulator-receivers for integrated full-duplex wireless. *IEEE Journal of Solid-State Circuits*, 53(8):2190–2201, 2018.

[63] Mahmood Baraani Dastjerdi, Sanket Jain, Negar Reiskarimian, Arun Natarajan, and Harish Krishnaswamy. 28.6 full-duplex 2×2 mimo circulator-receiver with high tx power handling exploiting mimo rf and shared-delay baseband self-interference cancellation. In *2019 IEEE International Solid- State Circuits Conference - (ISSCC)*, pages 448–450, 2019.

[64] R. Weinstein. Rfid: a technical overview and its application to the enterprise. *IT Professional*, 7(3):27–33, 2005.

[65] Edward A Keehr. A low-cost, high-speed, high-resolution, adaptively tunable microwave network for an sdr uhf rfid reader reflected power canceller. In *2018 IEEE International Conference on RFID (RFID)*, pages 1–8. IEEE, 2018.

[66] Sung-Chan Jung, Min-Su Kim, and Youngoo Yang. A reconfigurable carrier leakage canceler for uhf rfid reader front-ends. *IEEE Transactions on Circuits and Systems I: Regular Papers*, 58(1):70–76, 2010.

[67] Aravind Nagulu, Andrea Alù, and Harish Krishnaswamy. Fully-integrated non-magnetic 180nm soi circulator with > 1w p1db, >+50dbm iip3 and high isolation across 1.85 vswr. In *2018 IEEE Radio Frequency Integrated Circuits Symposium (RFIC)*, pages 104–107, 2018.

[68] Roman Trüb and Lothar Thiele. Increasing throughput and efficiency of lorawan class a. In *UBICOMM 2018. The Twelfth International Conference on Mobile Ubiquitous Computing, Systems, Services and Technologies*, pages 54–64. International Academy, Resarch, and Industry Association (IARIA), 2018.

[69] T. Polonelli, D. Brunelli, and L. Benini. Slotted aloha overlay on lorawan - a distributed synchronization approach. In *2018 IEEE 16th International Conference on Embedded and Ubiquitous Computing (EUC)*, pages 129–132, Los Alamitos, CA, USA, oct 2018. IEEE Computer Society.

[70] Rajeev Piyare, Amy L Murphy, Michele Magno, and Luca Benini. On-demand lora: Asynchronous tdma for energy efficient and low latency communication in iot. *Sensors*, 18(11):3718, 2018.

[71] A. Dongare, R. Narayanan, A. Gadre, A. Luong, A. Balanuta, S. Kumar, B. Iannucci, and A. Rowe. Charm: Exploiting geographical diversity through coherent combining in low-power wide-area networks. In *2018 17th ACM/IEEE International Conference on Information Processing in Sensor Networks (IPSN)*, pages 60–71, 2018.

[72] Rashad Eletreby, Diana Zhang, Swarun Kumar, and Osman Yağan. Empowering low-power wide area networks in urban settings. In *Proceedings of the Conference of the ACM Special Interest Group on Data Communication*, SIGCOMM '17, page 309–321, New York, NY, USA, 2017. Association for Computing Machinery.

[73] Akshay Gadre, Revathy Narayanan, Anh Luong, Anthony Rowe, Bob Iannucci, and Swarun Kumar. Frequency configuration for low-power wide-area networks in a heartbeat. In *17th USENIX Symposium on Networked Systems Design and Implementation (NSDI 20)*, pages 339–352, Santa Clara, CA, February 2020. USENIX Association.

[74] Mehrdad Hessar, Ali Najafi, and Shyamnath Gollakota. Netscatter: Enabling large-scale backscatter networks. In *16th USENIX Symposium on Networked Systems Design and Implementation (NSDI 19)*, pages 271–284, Boston, MA, February 2019. USENIX Association.

[75] Muhammad Osama Shahid, Millan Philipose, Krishna Chintalapudi, Suman Banerjee, and Bhuvana Krishnaswamy. Concurrent interference cancellation: decoding multi-packet collisions in lora. In *Proceedings of the 2021 ACM SIGCOMM 2021 Conference*, pages 503–515, 2021.

[76] Qian Chen and Jiliang Wang. Alignttrack: Push the limit of lora collision decoding. In *2021 IEEE 29th International Conference on Network Protocols (ICNP)*, pages 1–11. IEEE, 2021.